16th World Conference on Earthquake, 16WCEE 2017
Santiago Chile, January 9th to 13th 2017
Paper N° 2767 (Abstract ID)
Registration Code: S-C1463171548

Fragility of Low-Rise Moment Resisting Steel Frame Building Subjected to Crustal and Subduction Earthquakes

M. Bosco[(1)], L. Tirca[(2)]

[(1)]Associate researcher, Department of Building, Civil and Environmental Engineering, Concordia University, Montreal, Canada, Melina.Bosco@concordia.ca
[(2)]Associate professor, Department of Building, Civil and Environmental Engineering, Concordia University, Montreal, Canada, Lucia.Tirca@concordia.ca

Abstract

Performance-based earthquake engineering (PBEE) requires accurate estimation of the seismic demand on structures. Implementation of PBEE in quantitative evaluation of the performance of a given building is denoted here as Performance-Based Assessment (PBA). The methods used to tackle this task are incremental dynamic analysis (IDA), fragility analysis, and collapse safety verification where both epistemic and aleatoric uncertainties were considered.

The purpose of this study was to investigate the performance of low-rise steel moment resisting frame (MRF) office building located in Vancouver, B.C., Canada under earthquake shaking, to identify the maximum interstorey drift and residual interstorey drift, as well as, to derive fragility curves for life safety (LS) and collapse prevention (CP) performance levels. In addition, the proposed equation for predictive maximum residual interstorey drift provided in FEMA P 58-1 (2012) was verified. It is noted that steel moment resisting frame buildings undergoing residual interstorey drift larger than 1.0% h_s (where h_s is the storey height) are proposed for demolition rather than repair. In this paper, a comparative analysis is conducted in order to investigate the collapse margin safety of studied building subjected to crustal versus subduction ground motions.

The case study is a prototype 4-storey moderately ductile MRF office building located on Site Class C in Vancouver B.C., Canada. The building structure was designed according to the 2010 edition of National Building Code of Canada and the steel design standard CSA/S16-09. For simulating the nonlinear response from yielding to failure, a refined plastic hinge model able to consider strength and stiffness degradation caused by the low-cycle fatigue was developed in the OpenSees framework (Open System for Earthquake Engineering Simulation). The proposed model was validated against 16 experimental test results found in the literature. In this study, fragility curves were derived from the incremental dynamic analysis curves (IDA). To assess the damage state on the IDA curves, the maximum interstorey drift and maximum residual interstorey drift were recorded for each level of earthquake intensity. In addition, a damage index was proposed in order to trigger the ductile-fracture induced failure in cross-section fibers of a W-shape beam's plastic hinge zone.

From analyses it was found that the nonlinear response was mostly influenced by the number of loading/ unloading cycles with large amplitudes and the Trifunac duration. Hence, the interstorey drift limit of 5.0% h_s proposed for the CP limit state in FEMA 273 (1997) and FEMA 356 (2000) was found to be slightly overestimated when the low-rise MD-MRF building was subjected to subduction ground motions and too conservative in the case of crustal ground motions. The average value of ajusted collapse margin ratio (ACMR) of studied MD-MRF building was larger than the minimum permissible value corresponding to 10% probability of collapse ($ACMR_{10\%}$) under both sets of ground motions; hence it fulfils the collapse safety margin criteria. As expected, larger collapse margin ratio resulted in the case of building subjected to crustal ground motions than subduction records. Regarding the verification of the predicted median residual interstorey drift equation given in FEMA P 58-1 (2012), it was found that for the CP performance level, the median predicted residual interstorey drift was underestimated by about 20% for both crustal and subduction records.

Keywords: performance based assessment; steel moment resisting frame; nonlinear time-history analysis; IDA curves.

1. Introduction

The Pacific coast of Canada and more specifically the province of British Columbia (BC) is susceptible to crustal and subduction earthquakes. About 90% of earthquakes recorded in the region of Vancouver, BC, occurred in the continental crust (crustal earthquakes) [1]. Due to the vicinity of the Cascadia subduction fault, the building stock in Vancouver is vulnerable to subduction earthquakes, too. Thus, the main contributions to seismic hazard are the moderate to large crustal earthquakes of magnitudes 6.5 to 7.5 and the Cascadia subduction earthquake with a predicted moment magnitude M_w in the range of 8 to 9 and a recurrence period of 500 years [2]. The characteristics of subduction versus crustal ground motions vary in terms of amplitude, Trifunac duration, and frequency content.

In this study, the Performance-Based Assessment of a low-rise moderately ductile moment resisting frame (MD-MRF) prototype office building located in Vancouver, BC, Canada, is carried out. To tackle this task, the incremental dynamic analysis method (IDA) is employed and both sets of crustal and subduction ground motions selected and scaled to match the geotechnical profile for Site Class C (firm soil) in Vancouver, BC are considered. Further, fragility curves are derived from the incremental dynamic analysis curves (IDA) and both epistemic and aleatoric uncertainties are taken into account. Using a refined numerical model developed in OpenSees [3], the collapse safety of the studied building is also investigated.

2. Case Study

To assess the performance of a low-rise steel building subjected to crustal and subduction ground motions, a prototype 4-storey moderately ductile moment resisting frame (MD-MRF) office building located on firm soil (Site Class C) in Vancouver, B.C. is considered. The plan view of the building is shown in Fig. 1a. As illustrated, the seismic force resisting system consists of four identical MD-MRFs of three bays each displaced in the N-S direction and two MD-MRFs of five bays each located in the E-W direction. The height of ground floor level is 4.5 m and that of typical floor is 3.8 m. All MD-MRFs columns are continuous over the building's height and are fixed at the base. For example, in Fig. 1a, the side columns and the middle columns of MD-MRF 2 are labeled Type 1 and Type 2, respectively. All gravity columns are pinned at the base, and are labeled Type 3.

The studied building is designed according to NBCC 2010 [4] and CSA/S16-09 standard [5] provisions. The magnitude of dead load at the roof (DL_{roof}) and typical floor level (DL_{typ}) is equal to 3.0 kPa and 4.7 kPa, respectively. The snow load (SL) is equal to 1.8 kPa, the live load at typical floor (LL) is 2.4 kPa and the dead load due to cladding walls is 1.0 kPa. At building location, the design spectral ordinates *S(T)* at 0.2, 0.5, 1.0, and 2.0 s are 0.94, 0.64, 0.33, 0.17*g* where *g* is the gravitational acceleration. For seismic design, the load combination is: DL + 0.5 LL + 0.25 SL + E. According to [4], the static base shear, *V*, is computed as:

$$V = \frac{S(T_a) M_V I_E W}{R_d R_0} \tag{1}$$

where $S(T_a)$ is the 5% damped design spectral response acceleration corresponding to the fundamental period of vibration T_a, I_E is the importance factor for earthquake loads E, M_v is the factor accounting for higher mode effect on base shear, W is the seismic weight of the building which includes 25% of snow load, R_d and R_0 are the ductility-related and overstrength-related force modification factors, respectively. For the selected MD-MRF system, the values of the above parameters are: $R_d = 3.5$, $R_0 = 1.5$, $M_v = 1.0$ and $I_E = 1.0$.

For preliminary design, the fundamental period of the prototype 4-storey MD-MRF building was computed according to the code empirical equation $T_a = 0.085 h_n^{3/4}$, where h_n is the total building height (15.9 m). Applying this equation it leads to $T_a = 0.68$ s. Since the distribution of seismic internal forces is determined by the modal response spectrum analysis, the code allows amplifying the fundamental period T_a by a factor of 1.5 [4]. Thus, T_a is equal to1.02 s and the computed static base shear is $V = 2087$ kN. It is noted that the seismic weight of the building is $W = 33452$ kN. Further, the MD-MRF members were proportioned to carry the design base shear V_d resulted from modal response analysis which was scaled up to 0.8*V* as requires in [4]. In

this case study, the torsional effect was neglected, while the *P*-Δ effects were considered. Hence, the internal forces obtained from a first-order elastic analysis were amplified by the coefficient U_2 calculated as:

$$U_2 = 1 + \frac{\sum C_f R_d \Delta_f}{\sum V_f h} \quad (2)$$

where C_f is the factored gravity load, V_f is the storey shear and Δ_f is the relative first-order lateral displacement of the storey due to factored loads [5]. It is noted that an increase in stiffness (and consequently in strength) of structural members was required to reduce the value of coefficient U_2 under the prescribed limit of 1.4. The peak interstorey drift obtained from linear elastic analysis was within the code limit of 0.025 h_s, where h_s is the storey height. All the MD-MRF beam and column members are made of W-shapes with F_y = 350 MPa and F_u = 450 MPa. The storey seismic weight and the cross-section assigned to the MD-MRF 2 members are given in Table 1. The first-mode vibration periods of the structure along the *x*- and *y*- direction evaluated by eigenvalue analysis are T_{1x} = 2.03 s and T_{1y} = 2.15 s. As resulted, the code-based fundamental period T_a is lower than T_1. This finding was also reported in other studies. In light of this, Elkady and Lignos [6] concluded that the difference between the code-based fundamental period provided in ASCE/SEI 7-10 [7] provisions and the computed period from dynamic analysis is more pronounced for low-rise and middle-rise buildings than for high-rise buildings.

In this study, only the analysis in the N-S direction is provided. Due to building symmetry, all four MD-MRFs displaced in the N-S direction are identical. The numerical model developed for the MD-MRF displaced in gridline 2 is depicted in Fig. 1b. The stiffness of afferent gravity columns was also considered in the model.

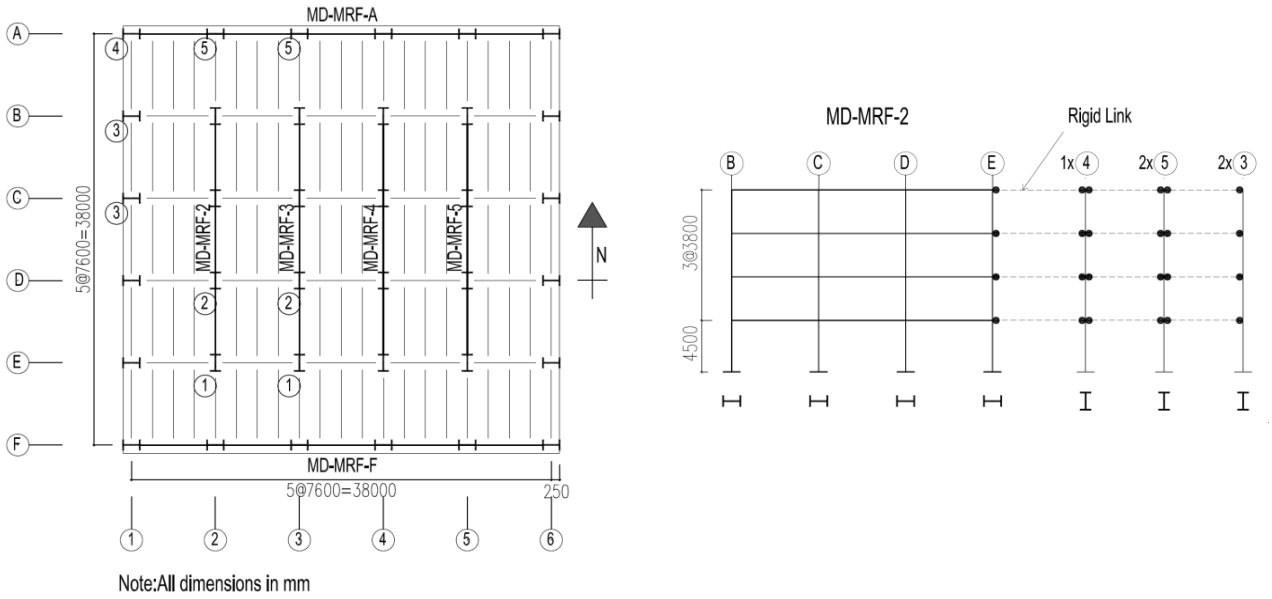

a) Plan layout b) N-S elevation model

Fig. 1 – Building studied

Table 1 – Storey seismic weight (kN) and MD-MRF 2 members' cross-sections

Storey	Seismic Weight	Beams	Column Type 1	Column Type 2
4	5462	W360x33	W360x91	W360x122
3	9330	W360x33	W360x91	W360x122
2	9330	W410x46	W460x128	W460x128
1	9338	W410x46	W460x128	W460x128

2.1. Ground Motion Selection and Characteristics

To analyze the seismic performance of the prototype 4-storey building, two sets of ground motion comprising crustal and subduction records have been considered. The first set consists of seven crustal ground motions selected from the PEER-NGA ground motion database, where NGA is the record identification given in Table 2. These records, suitable for Site Class C, originate from earthquakes with M_w6.9 and M_w6.7 and are characterized by an average shear wave velocity computed for the upper 30.0 m, V_{s30}, is in the range of $360 < V_{s30} < 760$ m/s. The second set consists of seven subduction records from the M_w9 Tohoku earthquake. It is noted that the best available proxy to a future Cascadia event are the main-shock records from the Tohoku, Japan earthquake of March 11, 2011. All ground motion records for the Tohoku earthquake were selected from the K-NET databases (http://www.kyoshin.bosai.go.jp/). As shown in Table 2, the main differences between the crustal and subduction records are the total earthquake duration, t, and the Trifunac duration, t_d, respectively. The mean ground motion period of subduction records is in the range of 0.2 s to 0.32 s and that of crustal records is in the range of 0.38 to 0.67 s. Details about the selection of Tohoku records are given in [8]. In accordance with the ASCE/SEI 7-10 [7] procedure, all ground motions were scaled such that the mean acceleration spectrum of minimum 7 records to match or be slightly above the design spectrum over the period of interest $0.2T_1 - 1.5T_1$. In Fig. 2 are illustrated the acceleration response spectrum of each individual ground motion, the mean spectrum of 7 ground motions and the design spectrum for Vancouver Site Class C. A scale factor equal to 1.0 was applied to all scaled subduction records.

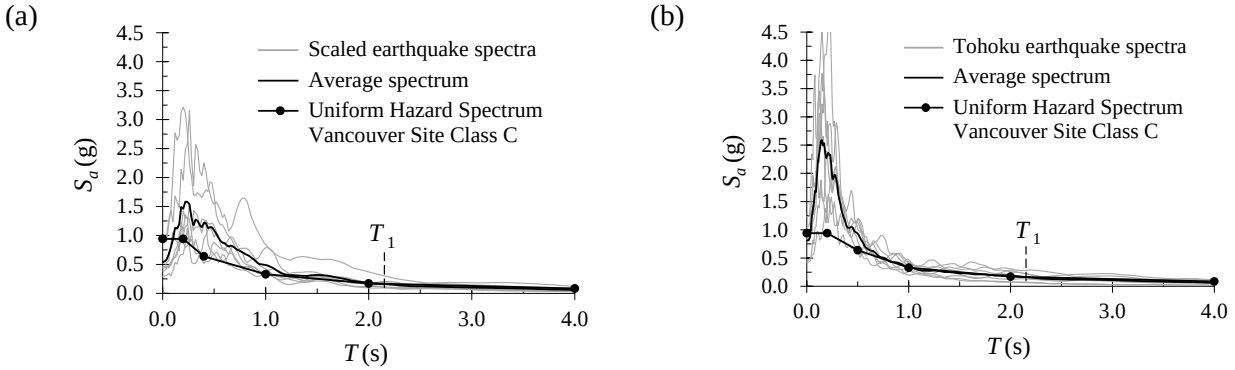

Fig. 2 – Scaled earthquake spectra: (a) crustal records, (b) subduction records

Table 2 – Ground motions

Records	NGA-Comp	Event	Mw	Station	t (s)	t_d (s)
Crustal ground motions						
C1	739-250	Loma Prieta	6.9	Anderson Dam (Downstream)	40.00	10.40
C2	767-000	Loma Prieta	6.9	Gilroy Array #3	39.94	6.37
C3	787-360	Loma Prieta	6.9	Palo Alto - SLAC Lab	39.57	11.58
C4	963-090	Northridge	6.7	Castaic, Old Ridge Route	45.00	9.08
C5	986-185	Northridge	6.7	LA - Brentwood VA Hospital	49.82	11.43
C6	1006-090	Northridge	6.7	LA - UCLA Grounds	60.00	11.30
C7	1039-180	Northridge	6.7	Moorpark - Fire Station	40.00	14.22
Subduction ground motions						
S1	MYG001	Tohoku	9.0	MYG001	300.0	83.0
S2	MYG004	Tohoku	9.0	MYG004	300.0	85.0
S3	FKS005	Tohoku	9.0	FKS005	300.0	92.0
S4	FKS010	Tohoku	9.0	FKS010	300.0	66.0
S5	FKS009	Tohoku	9.0	FKS009	300.0	74.0
S6	IBR004	Tohoku	9.0	IBR004	300.0	33.0
S7	IBR006	Tohoku	9.0	IBR006	300.0	36.0

3. Methodology

To assess the performance of studied low-rise MD-MRF office building, the seismic factors resulted from the building nonlinear responses are quantified according to FEMA P-695 [9] procedure. Herein, the nonlinear collapse simulation techniques are used to link seismic performance factors to system performance capabilities on a probabilistic basis. Accordingly, acceptable performance is achieved when the average value of adjusted collapse margin ratio, ACMR exceeds $ACMR_{10\%}$, where the latter is the minimum permissible ACMR value corresponding to 10% probability of collapse. However, to obtain the $ACMR_{10\%}$ value from tables provided in [9], the total system collapse unceertainty parameter, β_{TOT}, is required and need to be calculated. It is noted that uncertainty influences the shape of fragility curves plotted from incremental dynamic analysis results. In this study, fragility curves are derived from the IDA curves, which are carried out for each individual ground motion. Meanwhile, the building performance levels are defined on each IDA curve where the engineering demand parameter expressed in term of maximum interstorey drift among floors is plotted against the incremented intensity measure parameter defined by the spectral intensity of the building's first mode period.

According to ASCE/SEI 41-13 standard [10], the building performance levels are: operational (O), immediate occupancy (IO), life safety (LS), and collapse prevention (CP). In order to assess the building performance from yielding to failure, an accurate numerical model was developed in OpenSees. The IO performance level is reached when the first yielding occurs in the beam's plastic hinge. Herein, the LS performance level is defined at the critical limit state between the occurrence of peak residual interstorey drift of *1%* h_s and peak interstorey drift of *2.5%* h_s which is the code limit at the design level [4]. In this study, two criteria were considered to define the CP performance level: i) the sideway collapse associated with beams and columns hinging expressed by the peak interstorey drift from the IDA curves; and ii) the ductile-fracture induced failure which is measured by a damage index DI calculated for each beam cross-section within the plastic hinge zone. The computation of damage index DI is explained in the following section. According to [11], for steel moment resisting frames, the maximum interstorey drift/ residual interstorey drift associated to the CP performance level is 5.0% h_s. Although this interstorey drift limit may be conservative, it was adopted in this study. The reduction in MD-MRF beam capacity is expected to be dependent on the loading history and strongly correlated to the Trifunac duration.

4. Performance Assessment

4.1 Nonlinear Analysis Model

The elevation of numerical model depicted in Fig. 1b was developed for one quarter of the building due to building symmetry. This model comprising the MD-MRF 2 is simulated in the OpenSees software [3]. Herein, to reproduce the nonlinear response upon failure, the beam with hinges element was selected to replicate the behavior of all MD-MRF beams. In the case of beam with hinges, the yielding is spread along the hinge region where the moment-rotation response is expressed as a function of plastic hinge length and properties of fibers cross-section discretization parameters. The plastic hinge segments of W-shape beam cross-sections were made of fibers. Each flange of the W-shape cross-section was discretized into 40 x 4 fibers and the web into 20 fibers. The middle part of the beam with hinges element behaves elastically, while the plastic hinge segments made of *Steel02* material behave in the nonlinear range. Among various plastic hinge integration procedures, the modified Gauss-Radau hinge integration method, labelled *HingeRadau* in OpenSees, was adopted. In this case, plasticity is confined to a single integration point located at each end of the plastic hinge length [12]. In the proposed beam model, the ductile-fracture was triggered in the critical cross-section of beam's hinge zone. Hence, the degradation of stiffness and strength due to local buckling of flanges were simulated upon failure by wrapping the low-cycle fatigue material developed in OpenSees to *Steel02* material assigned to cross-section fibers of plastic hinge zone. This fatigue material uses an accumulative strain model to predict damage in accordance with the Miner's rule. The relation between the plastic strain amplitude experienced at each cycle and the number of cycles to failure is that proposed by Coffin and Manson. The fatigue ductility exponent m was considered constant and set as m = -0.5, while the predicted fatigue coefficient ε_0 assigned to flange's fibres has a linear distribution as proposed in [13]. The minimum predicted value $\varepsilon_{0,min}$ was assigned to the end segment of

flanges' fibers and the maximum predicted value ($\varepsilon_{0,min} + \Delta\varepsilon_0$) was assigned to flange's fibers located at the intersection with the web. While the $\varepsilon_{0,min}$ value is related to the initiation of local buckling, the term $\Delta\varepsilon_0$ controls the rate of degradation. These parameters were calibrated against 16 experimental test results found in the literature. Details about the calculation of the plastic hinge length, L_{pl}, and the fatigue parameters $\varepsilon_{0,min}$ and $\Delta\varepsilon_0$ are provided in [13]. For each cross-section within the W-shape beam's plastic hinge zone a damage index DI was calculated. This DI is computed as the ratio of the number of flanges fibers in which the Miner's damage index is equal to one (i.e. the number of fibres reaching fatigue) to the entire number of flanges fibers within a given cross-section. When DI = 1.0, flanges of W-shape beam's cross-section are not able to sustain the bending moment developed in the plastic hinge zone. A value of DI = 0.375 has been proposed in [13] as an index of beam failure caused by low-cycle fatigue. This value corresponds to approximately 80% of remained bending moment capacity. Further, it is noted that the beam with hinges element defined in OpenSees does not account for shear deformability of the beam. To overcome this drawback, one vertical spring was added at each end of the beam as reported in [14]. Each column belonging to the MD-MRF was modelled with 8 nonlinear beam-column elements with distributed plasticity. An initial camber of 0.1% of the column height was applied at the column mid-height and all column members were made of *Steel02* material. All gravity columns were modelled with elastic elements.

In this study, two collapse modes were considered: i) sideway collapse associated with beams and columns hinging conducted to excessive interstorey drift on IDA curves; and ii) ductile-fracture in one of the beam's hinge region caused by low-cycle fatigue. Further, in the definition of CP limit state, the model is able to capture the nonlinear response until the point at which ductile-fracture occurred in the first beam's plastic hinge, while the beam-column connections remain undamaged. However, in the calculation of beam stiffness the contribution of the composite floor slab is not included, while for each beam and column, the model yield point is defined by the plastic moment capacity M_p calculated with the expected steel yield strength value equals to $1.1F_y$. The contribution of the gravity frame was considered in the model.

4.2 IDA Curves

IDA curves are computed for each individual ground motion [15]. Each point of the IDA curve obtained for a given ground motion relates the peak interstorey drift resulting from nonlinear time-history analysis to the spectral intensity of the building's first mode period. The obtained IDA curves computed for both ground motion sets are shown in Fig. 3. In order to emphasize the critical collapse mode, white circles are plotted on each IDA curve to mark the spectral acceleration corresponding to the first achievement of DI = 0.375 in the cross-section of a beam's plastic hinge zone. The cross-shape symbol marks the spectral acceleration corresponding to the referred interstorey drift of 5.0% h_s and the grey circle shows the spectral acceleration corresponding to a peak residual interstorey drift among floors of 1.0% h_s. Based on the IDA concept, the collapse is defined when for a small increase of intensity measure parameter it results a large increase of engineering demand parameter (i.e. interstorey drift) materialized by a flat line on the IDA curve. This point on the IDA curve is characterize by convergence problem and is marked with a triangle symbol. The design spectral acceleration corresponding to 2% in 50 years probability of exceedance is 0.16 g and is showed in Fig. 3 by a horizontal dashed line.

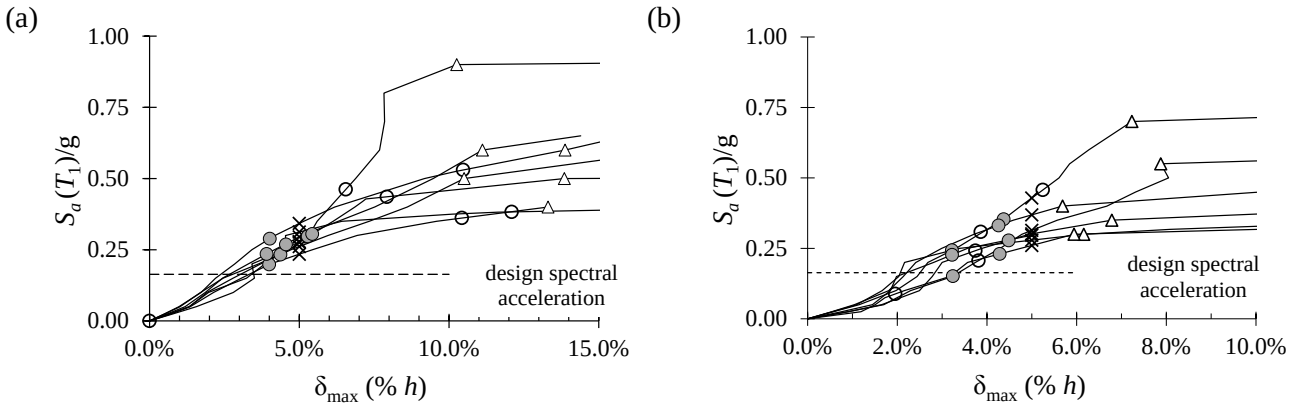

Fig. 3 – IDA curves: (a) crustal records, (b) subduction records

The LS performance level is defined on each set of IDA curves by the most critical of the followings: the residual interstorey drift of 1.0% h_s or an interstorey drift of 2.5% h_s computed for each set of 7 records. As depicted, the achievement of residual interstorey drift equal to 1.0% h_s occurs for ground motion intensities larger than those corresponding to interstorey drift equal to 2.5% h_s. This finding does not depend on the record's type. The peak interstorey drift at each floor and the associated residual interstorey drift corresponding to the LS performance level are depicted for each ground motion in Figs. 4 and 5. As illustrated, the maximum interstorey drift occurs at the top floor. As an average, the LS is reached for a value of the spectral intensity of the building's first mode period equal to 0.13 g for crustal records and 0.15g for subduction records.

The CP performance level is reached for a maximum interstorey drift greater than 5.0% h_s when crustal records are considered. Conversely, when subduction records are employed, the CP performance level is reached for interstorey drifts lower than 5.0% h_s for four out of seven records. As a consequence, a greater variability of the spectral acceleration at collapse is expected. Thus, the interstorey drift limit of 5.0% h_s proposed for the CP limit state in [11] is slightly overestimated when the low-rise MD-MRF building is subjected to subduction ground motions and is too conservative in the case of crustal ground motions. Meanwhile, in the case of subduction ground motions, the mean rotation value corresponding to DI = 0.375 is 0.058 radians. Figs. 6 and 7 show the distribution of interstorey and residual interstorey drift corresponding to CP performance level as defined above. As depicted, for crustal ground motions, the maximum interstorey drift of 5.0% h_s occurred at top floor. When subduction records are considered, the maximum interstorey drifts are in the range of 2.0% h_s to 5.0% h_s. These values of drift are scattered because for some accelerograms the local collapse of beam's cross-section prematurely occurs. However, the associated residual interstorey drift is lower than 2.5% h_s.

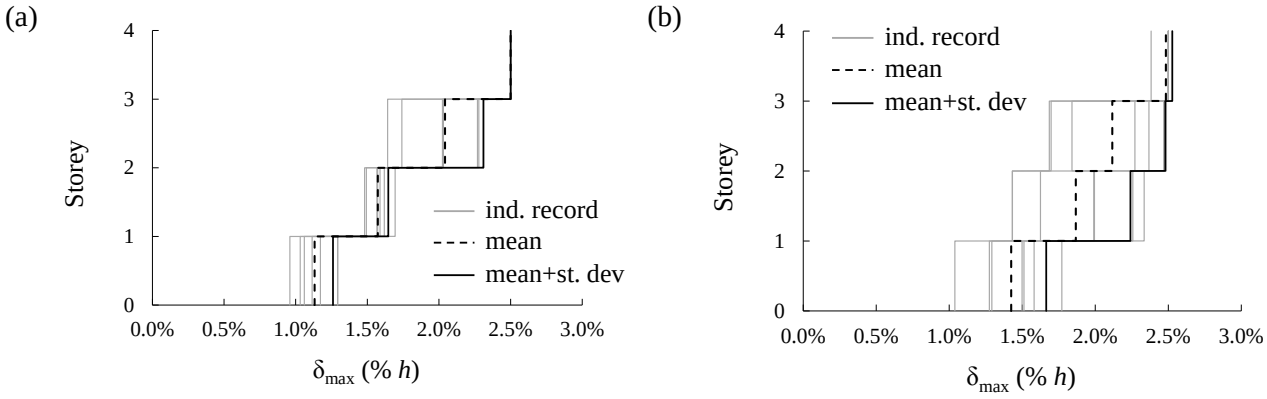

Fig. 4 – Interstorey drift at LS performance level: (a) crustal records, (b) subduction records

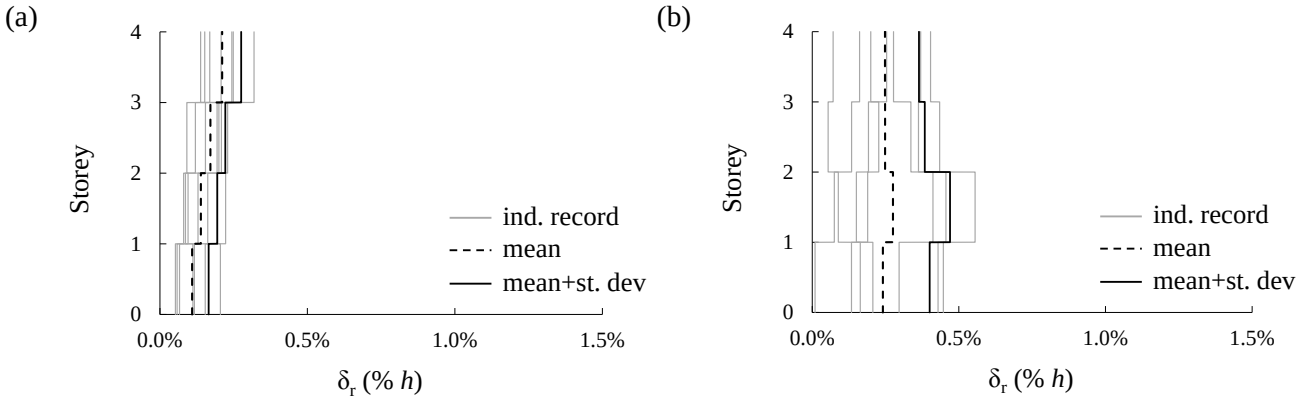

Fig. 5 – Residual interstorey drift at LS performance level: (a) crustal records, (b) subduction records

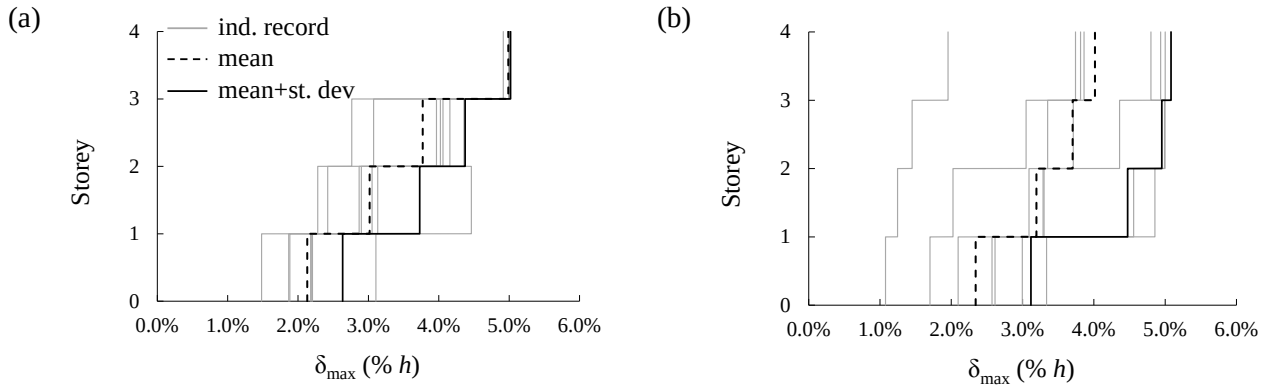

Fig. 6 –Interstorey drift at CP performance level: (a) crustal records, (b) subduction records

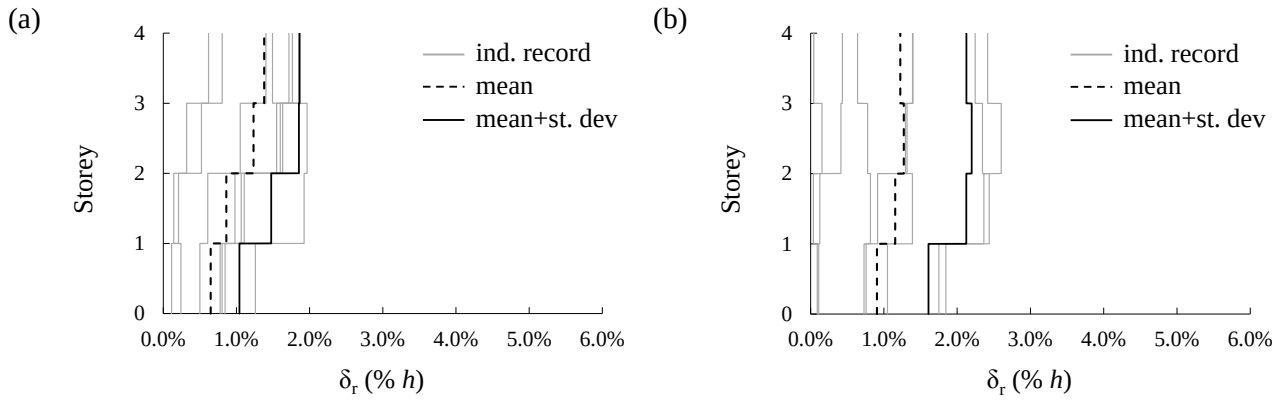

Fig. 7 – Residual interstorey drift at CP performance level: (a) crustal records, (b) subduction records

4.3 Fragility Curves

In this study, fragility functions were derived from parameters estimated using IDA curves [16]. The lognormal cumulative distribution function is used to define the fragility function, thus, the probability that a ground motion with an intensity measure IM =*x* will exceed a given performance level is:

$$P(\mathrm{PL} \mid \mathrm{IM} = x) = \Phi\left[\frac{\ln(x/m_R)}{\beta_R}\right] \tag{3}$$

where Φ is the standard normal cumulative distribution function, m_R is the median of the fragility function (i.e the IM level with 50% probability of exceeding the given PL) and β_R is the logarithmic standard deviation. It is noted that if the value of parameters m_R and β_R are obtained for the performed dynamic analyses, they only measure the aleatoric uncertainty in the structural seismic capacity (record-to-record uncertainty). Additional sources of uncertainty in estimating capacity are epistemic uncertainties (knowledge-based) which originate from assumptions formulated in analysis and from limitations in the supporting database. According to the procedure stipulated in [9], the epistemic uncertainties include the design requirements uncertainty (β_{DR}), the test data uncertainty (β_{TD}) and the modelling uncertainty (β_{MDL}). The design requirements uncertainty is related to the completeness and robustness of the design requirements, and the test data uncertainty is related to the completeness and robustness of the test data used to define the system. Modelling uncertainty is related to the accuracy of analysis model and its capability of capturing structural collapse through direct simulation or non-simulated component checks.

The epistemic uncertainties could be included in the fragility curves if the value of β_R in Eq. (3) is replaced by the total system collapse uncertainty parameter:

$$\beta_{TOT} = \sqrt{\beta_R^2 + \beta_{DR}^2 + \beta_{TD}^2 + \beta_{MDL}^2} \quad (4)$$

In order to evaluate the record-to-record uncertainty, the following relationship was established between the spectral acceleration at the fundamental period of the frame and the corresponding peak interstorey drifts [17].

$$\delta_{max} = a\, S_a^b(T_1) \cdot \varepsilon \quad (5)$$

where ε is a lognormal random variable with median 1.0 and logarithmic standard deviation $\sigma_{\ln\varepsilon}$ depicting the uncertainty β_R. The parameters *a*, *b* and ε were determined by regression of $ln\ \delta_{max}$ versus $ln\ S_a(T_1)$ as shown in Fig. 8. To calculate the total system collapse uncertainty the following assumptions are made: β_{DR} = 0.1 ("A-Superior" quality), β_{TD} = 0.2 ("B-Good" quality), β_{MDL}= 0.2 ("B-Good" quality). Thus, the total uncertainty is 0.362 for the crustal records and 0.399 for the subduction records. Two fragility curves obtained for the CP performance level under crustal and subduction records are shown in Fig. 9. One curve is derived by considering only the record-to-record uncertainty and the other one by considering the total system collapse uncertainty. The median collapse capacity $\overline{S}_a(T_1)$ derived from the fragility curves (i.e. the value at which 50% of ground motions produced building collapse) is equal to 0.284 g for the crustal records and 0.242 g for the subduction records.

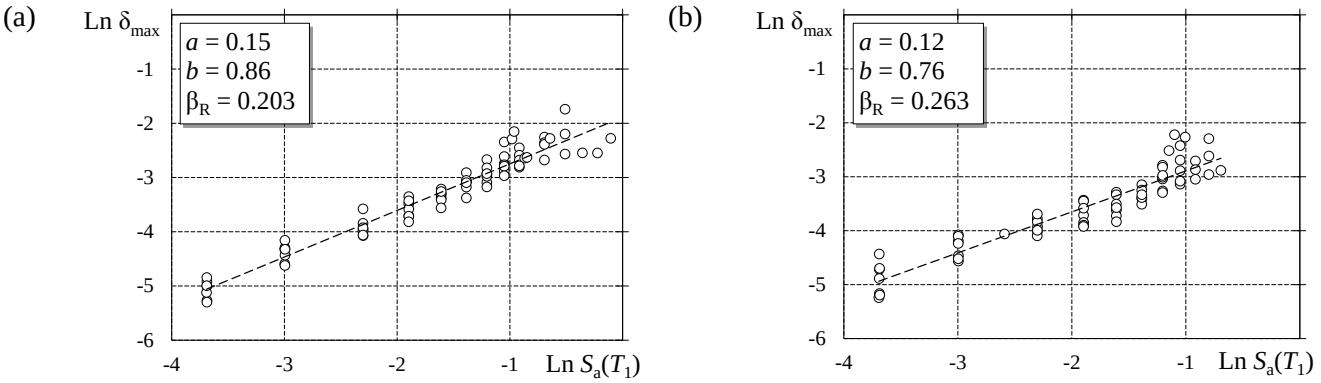

Fig. 8 – Regression analysis: (a) crustal records; (b) subduction records

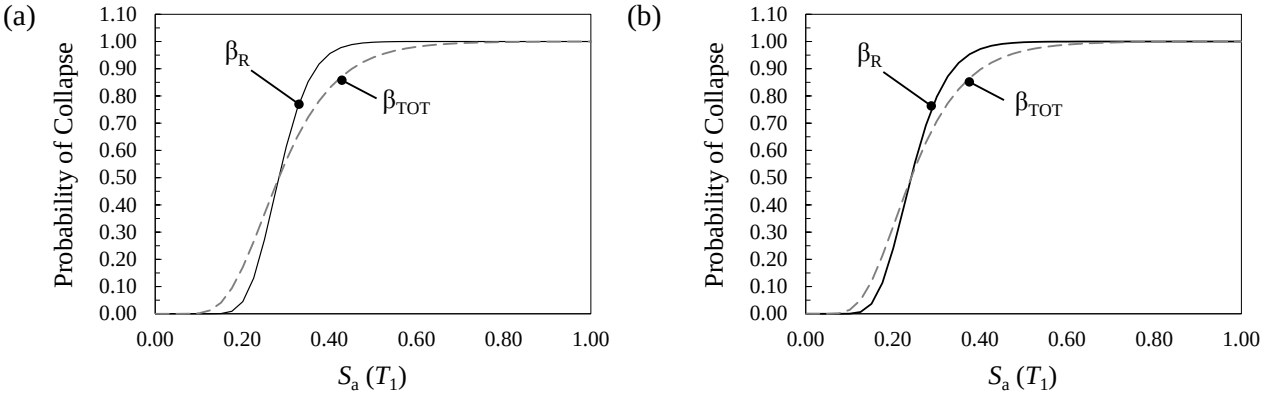

Fig. 9 – Fragility curve: (a) crustal records; (b) subduction records

4.4 Assessment of Collapse Safety

To assess the collapse safety according to FEMA P695[9] procedure it requires to evaluate the following quantities: (i) the collapse margin ratio (CMR), (ii) the spectral shape factor (SSF), and (iii) the adjusted collapse margin ratio (ACMR=CMR x SSF). To meet the collapse safety requirement, the ACMR of the studied building

has to be greater than $ACMR_{10\%}$, which is the minimum permissible ACMR corresponding to 10% probability of collapse. The $ACMR_{10\%}$ value is given in tables provided in [9] as a function of β_{TOT}.

The collapse margin ratio, CMR, is defined as the ratio between the median collapse capacity $\overline{S}_a(T)$ and $S_a(T_1)$, where $S_a(T_1)$ is the 2%/50 years design spectral acceleration ordinate at the first-mode period of building structure T_1. The CMR is significantly influenced by the frequency content (spectral shape) of ground motions. This effect is incorporated into the ACMR parameter as provided in [9]. The SSF factor depends on the first-mode period of studied structure and on the period-based ductility factor μ_T which is calculated from a nonlinear static procedure. A distribution of lateral forces proportional to the shape of the first mode of vibration of the structure is applied. The pushover analysis was stopped either when the roof displacement value δ_u corresponded to 20% strength loss (V=0.8V_{max}) as per [9] or when the interstorey drift equated 5% h_s (Fig. 10). The μ_T parameter is given in Eq. (6) and is calculated as the ratio between δ_u and $\delta_{y,eff}$, where the latter is the effective yield roof displacement given in Eq. (7).

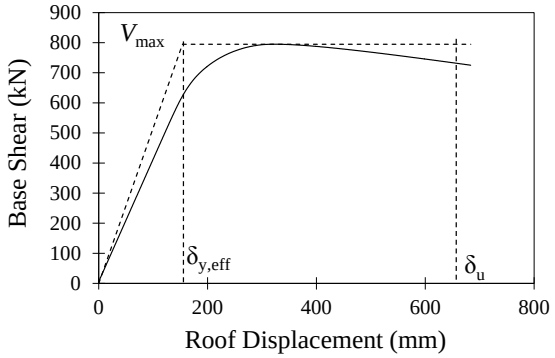

Fig. 10 – Pushover curve and definition of the period based ductility μ_T.

$$\mu_T = \frac{\delta_u}{\delta_{y,eff}} \tag{6}$$

$$\delta_{y,eff} = C_0 \frac{V_{max}}{W}\left(\frac{g}{4\pi^2}\right)\max(T_a;T_1)^2 \tag{7}$$

In the above equation, V_{max}/W is the maximum base shear normalised by the building weight and C_0 is the modal participation factor. For the structure under examination, μ_T is equal to 4.40 and the SSF is equal to 1.265. The obtained values of CMR, ACMR and $ACMR_{10\%}$ are provided in Table 3 for both sets of records. It is concluded that the studied structure fulfills the requirements given in [9], or more precisely ACMR > $ACMR_{10\%}$. However, the collapse safety margin is greater when building was subjected to crustal records rather than subduction records. Thus, the ACMR is 1.37 time greater than $ACMR_{10\%}$ when crustal records were considered and only 1.12 time greater in the case of subduction records. This finding is in agreement with that reported in [8].

Table 3 – Parameters for the assessment of collapse safety

Earthquake type	$S_a(\overline{T}_1)$	**CMR**	**ACMR**	β_{Tot}	$ACMR_{10\%}$	**Check**
Crustal	0.284 g	1.737	2.197	0.362	1.595	OK
Subduction	0.242 g	1.480	1.872	0.399	1.668	OK

4.5. Predicted versus Computed Residual Interstorey Drift

The maximum residual interstorey drift ratio is an index used to determine if the building is or is not reparable. However, the prediction of residual interstorey drift by nonlinear analysis is highly sensitive to modelling assumptions related to the postyielding hardening/softening slope and unloading response. Further, the requirements for direct simulation of residual interstorey drift are computationally complex and not practical for general implementation in practical design. To overpass this drawback, in [18] it is proposed a simple equation

to predict the median residual interstorey drift δ_r^{pred} as a function of the median peak interstorey drift δ_{max} calculated from the nonlinear response history analysis and the interstorey drift associated with the first yielding in the structure, δ_y:

$$\delta_r^{pred} = \begin{cases} 0 & \text{if } \delta_{max} \le \delta_y \\ 0.3 \cdot (\delta_{max} - \delta_y) & \text{if } \delta_y < \delta_{max} < 4\delta_y \\ (\delta_{max} - 3\delta_y) & \text{if } \delta_{max} \ge 4\delta_y \end{cases} \quad (8)$$

In this study, the above equation is verified at the LS and CP performance levels. Herein, δ_y is evaluated from the IDA curve as the median interstorey drift corresponding to the first achievement of bending moment equal to the factored moment resistance, while the median of maximum interstorey drifts δ_{max} referres to Figs. 4 and 6. The median of maximum residual interstorey drifts δ_r are calculated from the nonlinear dynamic analysis and are associated to Figs. 5 and 7. Then, by using Eq. (8), the predicted median residual interstorey drift values δ_r^{pred} are calculated. All obtained values are listed in Table 4. Thus, for the LS performance level, the median predicted residual interstorey drift is slightly greater than that computed under the effect of subduction ground motions and about 150% greater in the case of crustal ground motions. In the case of CP performance level, the median predicted residual interstorey drift values are underestimated by about 20% for both crustal and subduction earthquakes.

Table 4 – Computed versus predicted median residual interstorey drift for LS and CP performance levels

Earthquake type	**IO**	**LS performance level**			**CP performance level**		
	δ_y	δ_{max}	δ_r^{pred}	δ_r	δ_{max}	δ_r^{pred}	δ_r
Crustal	1.31%	2.50%	0.36%	0.22%	5.00%	1.10%	1.34%
Subduction	1.20%	2.41%	0.33%	0.27%	3.89%	0.77%	0.95%

5. Conclusions

The main conclusions of this study are:

1. The nonlinear seismic response of a 4-storey MD-MRF office building subjected to crustal and subduction records differs in several aspects and is mostly influenced by the number of loading/ unloading cycles with large amplitudes and the Trifunac duration. The damage state triggered at LS and CP performance levels is discussed.
2. The importance of a proper modelling of stiffness and strength degradation upon failure caused by low-cycle fatigue is higher when the building is subjected to subduction earthquake records. In this study, the MD-MRF beams were modelled with the beam with hinges elements with fibers cross-section discretization within the plastic hinge zone. Herein, the modified Gauss-Radau hinge integration method, labelled *HingeRadau* in OpenSees, was adopted and a refined low-cycle fatigue model calibrated against 16 experimental test results found in the literature was assigned to fibers of W-shape beam flanges within the plastic hinge zone.
3. The interstorey drift limit of 5.0% h_s proposed for the CP limit state in [11] is slightly overestimated when the low-rise MD-MRF building is subjected to subduction ground motions and is too conservative in the case of crustal ground motions. From IDA curves, it resulted that a mean residual interstorey drift of 1.0% h_s is associated with a mean interstorey drift of about 4% h_s under both sets of ground motion. When the MD-MRF building was subjected to subduction ground motion set, the ductile-fracture induced failure occurred for a mean interstorey drift of around 4.3% h_s and in the case of crustal ground motions it corresponds to a mean interstorey drift two times greater.
4. The average value of adjusted collapse margin ratio (ACMR) computed for the studied MD-MRF building exceeds the minimum permissible ACMR value corresponding to 10% probability of collapse ($ACMR_{10\%}$) under both sets of ground motion; hence it fulfils the collapse safety margin criteria. As expected, a larger collapse margin ratio resulted in the case of crustal ground motions than in that of subduction records.

5. Regarding the verification of the predicted median residual interstorey drift equation given in [18] it was found that for the LS performance level, the median predicted residual interstorey drift is slightly greater than that computed under the effect of subduction ground motions and about 150% greater in the case of crustal ground motions. In the case of CP performance level, the median predicted residual interstorey drift values are underestimated by about 20% for both crustal and subduction records.

6. Acknowledgements

Financial support for this study from the Natural Sciences and Engineering Research Council of Canada (NSERC) is gratefully acknowledged.

7. References

[1] Rogers GC (1994): Earthquake in the Vancouver area. *Geology and Geological Hazards of the Vancouver Region, Southwestern British Columbia*, (ed) J.W.H. Monger; Geological Survey of Canada, Bulletin 481, 221-229.

[2] Atkinson G and Goda K (2011): Effects of seismicity models and new ground-motion prediction equations on seismic hazard assessment for four Canadian cities, Bull. Seismol. Soc. Am. **101**, 176–189.

[3] McKenna F, Fenves G, Scott M, et al. (2015): Open system for earthquake engineering simulation. OpenSees software version 2.4.5, PEER, Univ. of California, Berkeley.

[4] National Research Council of Canada (NRCC). National Building Code of Canada (2010). NRCC, Ottawa, Canada.

[5] Canadian Standards Association (CSA). Limit States Design of Steel Structures, S16-09 Standard (2009). CSA, Toronto, Ontario, Canada.

[6] Elkady A and Lignos DG (2015): Effect of gravity framing on the overstrength and collapse capacity of steel frame buildings with perimeter special moment frames. *Earthquake Engineering & Structural Dynamics*, **44**, 1289–1307.

[7] ASCE. (2010). Minimum design loads for buildings and other structures. ASCE/SEI 7-10, Reston, VA

[8] Tirca L, Chen L, Tramblay R (2015): Assessing collapse safety of CBF buildings subjected to crustal and subduction eartquakes. *Journal of Constructional Steel Research*, **115**, 47-61.

[9] Federal Emergency Management Agency FEMA P-695 (2009): Quantification of building seismic performance factors, Washington, D.C.

[10] ASCE (2013): Seismic rehabilitation of existing buildings. ASCE/SEI 41-13, Reston, VA.

[11] Federal Emergency Management Agency FEMA 356 (2000): Prestandard and commentary for the seismic rehabilitation of buildings, Washington, D.C.

[12] Scott M and Fenves G (2006): Plastic hinge integration methods for force-based beam–column elements. *Journal of Structural Engineering*, ASCE, **132**(2), 244-252.

[13] Bosco M and Tirca L (2016): Numerical simulation of steel beam members using damage accumulation models. *Journal of Constructional Steel Research* (submitted).

[14] Bosco M, Marino EM and Rossi PP (2015): Modelling of steel link beams of short, intermediate or long length. *Engineering Structures*, **84**, 406–418.

[15] Vamvatsikos D, Cornell CA (2002): Incremental dynamic analysis. *Earthquake Engineering & Structural Dynamics*, **31** (3), 491-514.

[16] Baker JW (2015): Efficient analytical fragility function fitting using dynamic structural analysis. *Earthquake Spectra*, **31** (1), 579-599.

[17] Ellingwood B, Celik OC and Kinali K (2007): Fragility assessment of building structural systems in mid-America. *Earthquake Engineering & Structural Dynamics*, **36** (13), 1935–1952.

[18] Federal Emergency Management Agency FEMA P-58-1 (2012): Seismic Performance Assessment of Buildings, Vol. 1 Methodology, Washington, D.C.